

NUMERICAL SIMULATION OF FLOW AND HEAT TRANSFER THROUGH A TUNNEL KILN

Mônica F. Naccache

Pontifícia Universidade Católica do Rio de Janeiro, Rua Marquês de São Vicente 225, RJ 22453-900, Brazil
naccache@mec.puc-rio.br

Marcos S. P. Gomes

Pontifícia Universidade Católica do Rio de Janeiro, Rua Marquês de São Vicente 225, RJ 22453-900, Brazil
mospomes@mec.puc-rio.br

Angela O. Nieckele

Pontifícia Universidade Católica do Rio de Janeiro, Rua Marquês de São Vicente 225, RJ 22453-900, Brazil
nieckele@mec.puc-rio.br

Abstract. *In this work the flow and heat transfer of combustion gases inside a tunnel kiln are investigated numerically. This kind of furnace is used for red ceramic fabrication, originally with sawdust as fuel. The main goal of this work is to evaluate the use of natural gas instead of sawdust. The numerical solution was obtained by using a bi-dimensional approach, analyzing the flow in an horizontal plane of the original furnace. The numerical solution of the conservation equations of mass, momentum and energy was obtained using the finite volume method and the commercial software Fluent (Fluent Inc.), with a non-uniform structured mesh. Due to the high levels of temperature, radiation heat transfer was considered, and the DTRM (Discrete Transfer Radiation Model) model was used. The velocity, pressure and temperature fields inside the furnace were obtained and analyzed. The effects of porosity, permeability and gases inlet temperature were investigated and compared with experimental results from the literature. The results obtained show that natural gas can be used as a fuel for this type of furnace.*

Keywords: *ceramic furnace, heat transfer, natural gas*

1. Introduction

In the fabrication process of the red ceramic industry, the elements produced, such as bricks, are formed by an extrusion process, followed by a drying and a firing processes, which are performed inside a furnace unit. The tunnel kiln is the most widely firing unit used in the clay product industry. The tunnel kiln is a counter-flow kiln, where the pieces to be dried and fired are arranged on cars, which are continuously pushed in the opposite direction of the air and gases flow, coming from the combustion chambers. The tunnel kilns consist of three distinct zones: pre-heating, firing and cooling zones, each of them being 15-50 m long. The load enters the furnace at the pre-heating zone, where it is heated from the ambient temperature until a temperature level of 500-700°C. Heat is transferred to the load from the combustion gases coming from the firing zone, at high temperatures, and flowing counter-currently to the ware. The combustion gases flow to the chimney and exit the furnace at relatively low temperatures (100-150°C). The firing zone is the hottest kiln region, and is located between the pre-heating and the cooling zones. In the firing zone, the combustion gases enter the kiln, coming from the combustion chambers, and the ware is heated to the sintering temperature. In the cooling zone, the product is cooled by the pre-heating ambient air, until temperatures of 50-100°C. To provide a precise control of product temperature, the cooling zone can contain cold-air injections and hot-air extractions at different locations along it. The extracted hot-air can be used in other parts of the process, e.g. as combustion air in the firing zone.

The red ceramic industry is considered one of high energy consumption. In Brazil, most of them uses sawdust as fuel. However, this kind of fuel is becoming more expensive and difficult. Besides, the pollutant generation is also a great problem. Therefore, the seek for alternate fuels is increasing. Despite the fact that the kilns have been designed to operate with solid fuels, there is no problem in performing minor modifications so that the kiln would be able to operate with gas or liquid fuels. This work performs a numerical analysis in a simplified tunnel kiln, in order to evaluate the performance of the kiln using natural gas as fuel. Depending on the availability and price of the gas, its use may decrease the cost of energy consumption, and it reduces the pollutants emissions.

Some works have studied the thermal problem inside tunnel kilns. Carvalho and Nogueira (1997) performed a numerical study of this problem. Using experimental data, they showed that this is a good tool for the development of an optimization procedure to be used in the kiln design and operation. Abou-Ziyan (2004) obtained heat transfer coefficients and pressure drop data through a section of a tunnel kiln, for a wide range of Reynolds numbers, and different arrangements of bricks. The results showed that the pressure drop and convective heat transfer coefficient strongly depends on the setting pattern, and some correlations for Nusselt number were presented. Essenhigh (2001) performed an integral analysis of the energy equation through a tunnel kiln, to determine the relation between input energy and useful output energy. Santos (2001) presented a numerical formulation to obtain the thermal behavior of a

tunnel kiln, considering the heat transfer among its several components. Experimental data for a tunnel using sawdust as fuel were also obtained in order to evaluate the numerical results. A good agreement between the numerical and experimental results was obtained. Numerical simulations with natural gas were also performed to evaluate its use as fuel in this kind of kiln.

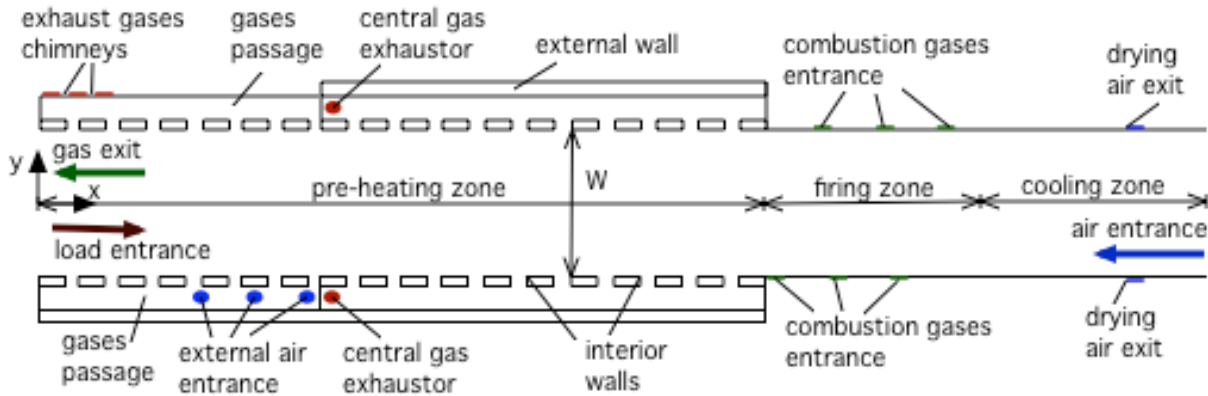


Figure 1. The furnace geometry

2. Mathematical Modeling

In order to analyze the thermal behavior inside a tunnel kiln, some simplifications were considered. The analysis was performed for a two dimensional situation, i.e., for a horizontal plane of the kiln, and a steady-state formulation was employed. The combustion process inside the combustion chambers was not analyzed in this work, and the load was considered as a homogeneous porous media. Figure 1 shows a scheme of the simplified geometry of the tunnel kiln, with the three different zones described before. In order to obtain the velocity, pressure and temperature fields, the governing conservation equations were solved, using a Cartesian coordinate system. The mass conservation equation is given by:

$$\text{div} (\rho \mathbf{v}) = 0 \quad (1)$$

where ρ is the density and \mathbf{v} is the velocity vector. The momentum conservation equation is:

$$\text{div} (\rho \mathbf{v} \mathbf{v}) = \rho \mathbf{g} - \text{grad } P + \text{div} (\mu \text{grad } \mathbf{v}) + \text{div} [\mu (\text{grad } \mathbf{v})^T] + S_{\text{por}} \quad (2)$$

where \mathbf{g} is the gravity vector, P is the pressure, μ is the viscosity and S_{por} is an extra source used to simulate the porous media (Fluent Users Guide, 2005). For a homogeneous porous media, the source term is given by:

$$S_{\text{por}} = - \left(\frac{\mu}{\alpha_{\text{perm}}} \mathbf{v} + C \frac{1}{2} \rho v_{\text{mag}} \mathbf{v} \right) \quad (3)$$

where α_{perm} is the permeability, v_{mag} is the modulus of the velocity vector and C is the inertial resistance factor, considered equal to zero, since the flow is too slow.

The energy conservation equation is given by:

$$\text{div} (\rho \mathbf{v} h) = \text{div} \left[\left(\frac{\mu}{\text{Pr}} \right) \text{grad } h \right] + \mathbf{v} \cdot \text{grad } \rho + \dot{q} \quad (4)$$

where $\text{Pr} = \mu c_p / k$ is the Prandtl number. The quantity \dot{q} is the enthalpy generation. In this problem, the enthalpy generation is only due to radiation ($\dot{q} = S_{\text{rad}}$). The enthalpy is given by:

$$h = \int_{T_{\text{ref}}}^T c_p dT \quad (5)$$

The heat conductivity of the porous media is equal to an effective heat conductivity, obtained by the following equation:

$$k_{ef} = \phi k_f + (1 - \phi) k_s \quad (6)$$

where k_f is the fluid heat conductivity, k_s is the solid heat conductivity and ϕ is the porosity, given by the ratio between the volume occupied by the fluid and the total volume of the porous media.

To obtain the enthalpy generation due to radiation, the Discrete Transfer Radiation Model (DTRM) (Carvalho et al., 1991) was employed. The main hypothesis of this model is that the radiation that leaves one surface, in a certain range of a solid angle, can be grouped in one direction or radius. It also neglects the effect of radiation spread caused by the medium. The radiation intensity variation dI through a distance ds , can be written by;

$$\frac{dI}{ds} + \alpha I = \frac{\alpha \sigma T^4}{\pi} \quad (7)$$

where α is the absorption coefficient, I is the total hemispheric intensity, T is the local temperature, and σ is the Stefan-Boltzmann constant, equal to $5,672 \times 10^{-8}$ Watts / $m^2 K^4$. The DTRM model integrate dI over a great number of radius, leaving from each surface of all control volumes. Therefore, the radiation intensity I is estimated as

$$I(s) = \frac{\sigma T^4}{\pi} (1 - \exp[-\alpha s]) + I_0 \exp[-\alpha s] \quad (8)$$

In the equation above, I_0 is the radiation intensity at $s=0$.

The absorption coefficient was calculated using the Weighted Sum of Gray Gases Model (WSGGM) (SmithShen, and Friedman, 1982), and it is locally given by

$$\alpha = \sum_{i=0}^I f_i a_i p \quad \text{if} \quad s \leq 10^{-4} \text{ m} \quad (9)$$

$$\alpha = -\ln(1 - \xi) / s \quad \text{if} \quad s \geq 10^{-4} \text{ m}$$

and

$$\xi = \sum_{i=0}^I f_i(T) [1 - \exp(-a_i p s)] \quad (10)$$

where f_i are the weight factors for the emissivity of the i -th gray gas, a_i are the absorption coefficients of the i -th gray gas, p is the sum of partial pressures of all participant gases, and ξ is the total emissivity in a distance s .

Boundary Conditions:

The boundary conditions are the impermeability and no slip conditions at walls, i.e., $u=v=0$. At the external walls, a convective heat loss was used, with the heat transfer coefficient equal to $10 \text{ W/m}^2\text{K}$. According to Figure 1, there are the following entrance regions:

- The ambient air entrance at the end of the kiln. At this boundary it was specified constant mass flow rate and temperature.
- Six inlets for the combustion gases coming from the combustion chambers, at the firing region, where it was given constant mass flow rate and constant temperature, which were defined by the solution of the combustion problem inside the combustion chamber.
- Three points for the entrance of external heated air at the pre-heating zone. At these points, source terms at the momentum and energy equations were used to take into account the air entrance

The exit regions were treated as follows:

- Two central gases exhaustors, where negative source terms at the momentum and energy equations were defined.
- Gas exit at the load entrance region: the flow was assumed fully developed.
- Nine exhaust gases chimneys: a negative constant velocity was used, assuming that 90% of the gases would flow through these chimneys (and the others 10% would exit through the tunnel entrance).

3. Numerical Solution

The flow field inside the kiln was numerically obtained using the FLUENT software (Fluent Inc.). The governing equations were discretized via finite volume method. The solution was considered converged when the sum of the normalized residuals of all equations was less than 10^{-3} .

As it was presented before, a bi-dimensional geometry was used, reproducing a horizontal plane of the kiln. The geometry dimensions are presented in Table 1, and the parameters used in the numerical simulation are shown in Table

2. An orthogonal mesh of 6368 control volumes was generated with the FLUENT auxiliary tool GAMBIT (Fluent, 2004).

4. Results and Discussion

In order to analyze the use of natural gas in the tunnel kiln, some results were obtained to compare with experimental results for a real tunnel kiln with sawdust as fuel, presented in Santos (2001). The geometry parameters used in the numerical simulations were based on this real tunnel kiln and are shown in Table 1.

Table 1. Geometry of the tunnel kiln used in the numerical simulation

Geometry	
Definition	Dimension
Kiln length	80m
Pre-heating zone length	36.5m
Firing zone length	11m
Cooling zone length	12m
Kiln interior wideness (W)	1,45m
Interior wall thickness	0.10m
Gases passage	0.25m
External wall thickness	0.15m
External wall thickness	1,25m
Interior walls length	0.75m
Distance between two interior adjacent walls	0.25m
Number of combustion furnaces	6
Combustion gases entrance wideness	0.23m
Distance between combustion gases entrance	3.45m
Number of exhaust gases chimneys	9
Exhaust gases chimneys wideness	0.5m
Position of chimney 1	0,5m
Position of chimney 2	3,5m
Position of chimney 3	6,5m
Position of chimney 4	9,5m
Position of chimney 5	12,5m
Position of chimney 6	15,5m
Position of chimney 7	18,5m
Position of chimney 8	21,5m
Position of chimney 9	24,5m
Position of external air entrance 1	14m
Position of external air entrance 2	20m
Position of external air entrance 3	26m
Position of external air entrance 4	32m
Drying air exit wideness	0.67m
Position of drying air exit	74m

The gases and air inlets were given in two different ways: as an inlet boundary or as a source term added to the conservation equations. According to Figure 1, the inlet conditions are:

- At the air entrance, it was given the air mass flow rate with a constant temperature ($\dot{m}_{ai} = 0.7692$ kg/s, $T_{ai}=300K$)
- At the six combustion gases entrance, it was given the mass flow rate at a constant temperature ($\dot{m}_{gi} = 0.0496$ kg/s, $T_{gi}=1070K$)
- At the external air entrances at the pre-heating zone, source terms were added to the conservation equations. The total mass source term is the mass flow rate obtained from the real case (equal to 1.1 kg/s). All the four entrances were considered equal. The momentum source term ($S = \dot{m}^2 / \rho A$) was calculated considering that the velocities are equal at both directions, and the energy source term was calculated using an estimated value for the temperature, $T=300$ K, at each region ($S = \dot{m} c_p T$).

The outlet conditions were treated as follows:

- At the gases exit, a developed flow condition was used, considering that only 10% of the gases would exit through this region. The remaining gases exit through the chimneys, where a negative velocity was set ($v = -0.537m/s$).
- At the drying air exits, in the cooling zone, it was specified a constant negative velocity, equal to -0.441 m/s.
- At the central gases exhaustors, negative source terms were set, and the outlet mass flow rate at each one was equal to $\dot{m}_{og} = 0.1875$ kg/s.

The following physical properties were considered. The absolute viscosity, specific heat and thermal conductivity of the gases were set equal to $\mu = 2.7 \times 10^{-5}$ Pa s, $c_p = 1200$ J/kgK and $k = 0.04$ W/(m K). The density,

specific heat and thermal conductivity of the ceramic material were set equal to $\rho = 1500 \text{ kg/m}^3$, $c_p = 1000 \text{ J/kgK}$ and $k = 0.04 \text{ W/(m K)}$. The density of the gases was calculated using the ideal gas law, $\rho = p_{op} / RT$, where $p_{op} = 1 \text{ atm}$ is the average operation pressure inside the furnace. The load inside the furnace was considered as a porous media. Different values of the porosity were analyzed, based on the load geometry. Another parameter of the medium is the permeability. Based on the geometry and flow parameters of the real case, permeability of the order of $2 \times 10^{-5} \text{ m}^2$ was found, but the influence of this parameter was also investigated. The load velocity inside the kiln is very low, so it was neglected in the simulations. The walls kiln material were ceramic, and a convective heat loss was considered, with the heat transfer coefficient equal to $10 \text{ W/m}^2\text{K}$.

Now some results are presented and discussed. The influence of entrance gases temperature, porosity and permeability of the porous media, in the temperature and velocity fields, was analyzed. Table 2 shows the cases investigated.

Table 2 – Cases Analyzed

Case	Entrance gases temperature (K)	Porosity	Permeability (m^2)
Case 1	1070	0,25	2×10^{-5}
Case 2	1070	0,10	2×10^{-5}
Case 3	1070	0,25	0,02
Case 4	1070	0,25	2
Case 5	1270	0,25	2×10^{-5}
Case 6	870	0,25	2×10^{-5}

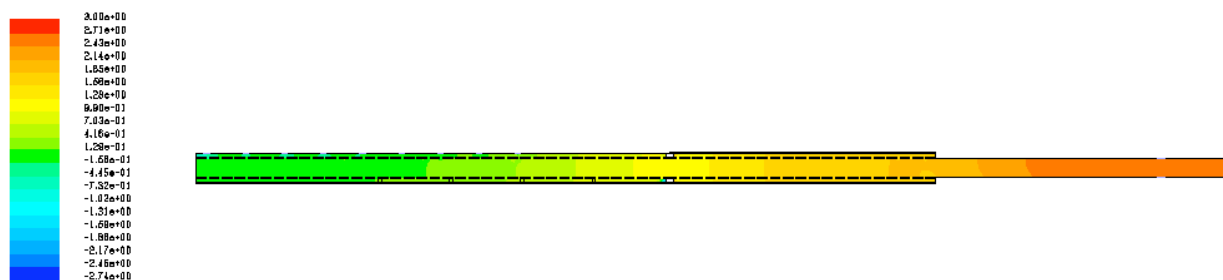


Figure 2 – Pressure field for Case 1

Figure 2 shows pressure field through the kiln. The pressure levels are relative to the atmospheric pressure. It can be noted that the pressure is almost invariant, which is in accordance to the experimental results obtained in Santos (2001). Figure 3 shows the velocity field for Case 1, where it can be observed that the higher velocity values are obtained in the middle and the end of the pre-heating zone, and in the firing zone, due to the combustion gases inlet. Near the load inlet and outlet, the velocities are lower, leading to lower heat transfer coefficients between the load and the gases.

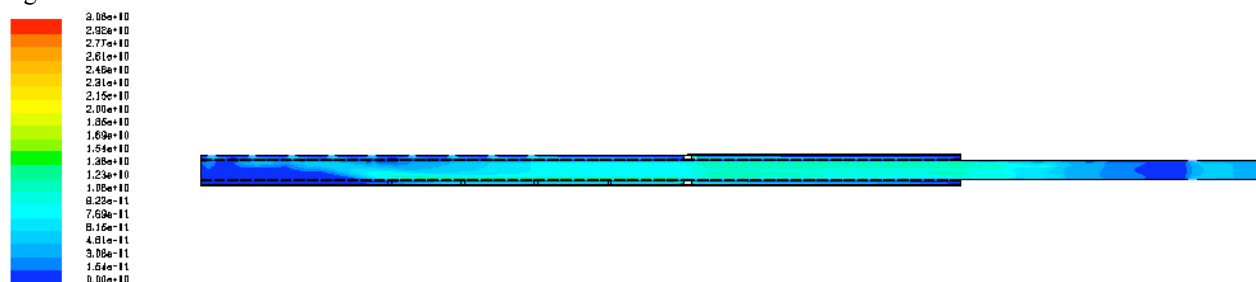


Figure 3. Velocity field for Case 1.

Figures 4 and 5 show the temperature field inside the kiln. It can be observed that at firing and pre-heating zones the temperature levels are higher, specially near the walls, where temperatures reach values of 800 K . At the central region of the pre-heating zone, lower values of temperature are found, due to the entrance of cold air.

Figure 6 shows the temperature variation at different axial positions: in two sections at the pre-heating zone ($x=20\text{m}$ and $x=47\text{m}$), and in one section at the firing zone ($x=62\text{m}$). It can be noted that at the colder region of the pre-heating zone, the temperature is almost constant, where at the other regions the temperature variations are larger, with higher temperatures near the walls and lower temperatures at the central regions.

Figure 7 presents the comparison between numerical and experimental results, the last ones obtained with sawdust as fuel (Santos, 2001). Figure 7 shows temperature through the kiln at two lateral positions, $y=0.55\text{m}$, which

corresponds to a position near the wall and at the center of the kiln, $y=1.225m$. The experimental results were obtained with termopars located at the right kiln wall, which can explain the better agreement between the numerical and experimental results at $y=0.55m$. However, it can be noted that there are some discrepancies even at this position, near the load exit ($x=70$ to $80m$) and at the central region ($x=20$ to $50m$), due to the approximations made at the numerical simulations. It can be observed that at the pre-heating zone (load entrance region) the temperatures are lower, as expected.

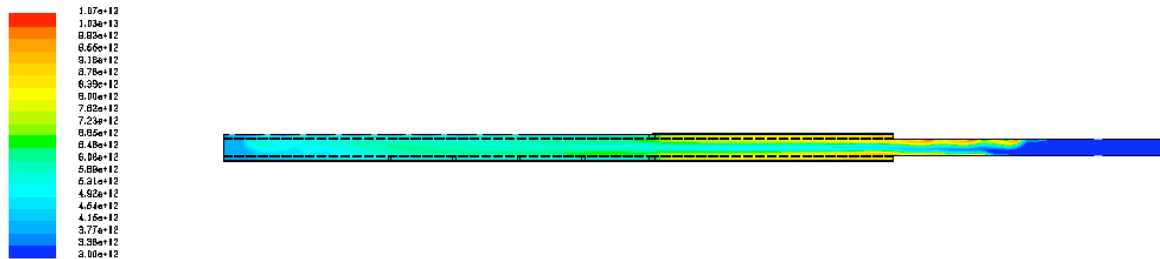


Figure 4. Temperature field inside the kiln

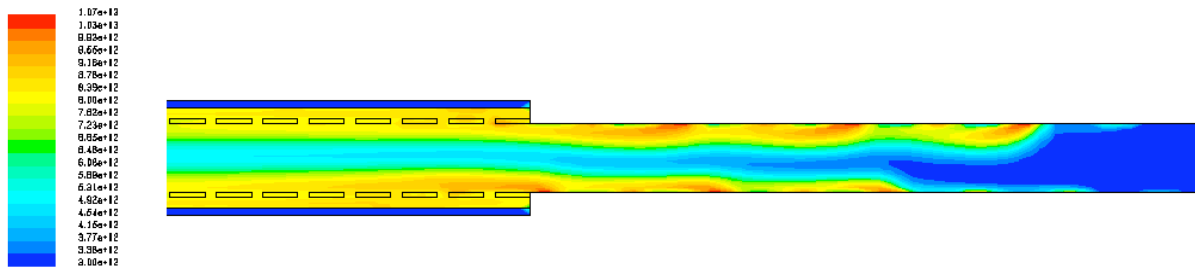


Figure 5. Temperature field at the firing zone.

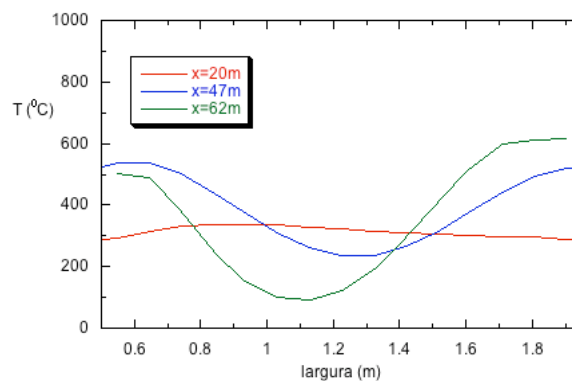


Figure 6. Temperature *versus* width at three axial positions, Case 1.

Figure 8 shows the temperature through the kiln at different transversal positions for the Case 1. It can be observed a large variation at the lateral section, with very low temperatures at the central region and high temperatures near the walls, indicating less efficient heating at the center of the kiln, due to low values of porosity and ceramic heat conductivity.

The effects of porosity and permeability on the temperature field are shown in Figs. 9 and 10. Figure 9 shows the influence of the load porosity (equal to 0.25 in Case 1 and 0.10 in Case 2). It can be noted that the results are very similar at this range of porosities, indicating that its effects are negligible. Figure 10 shows the comparison of results obtained with different values of the load permeability. It can be noted that its effect is also negligible.

Figure 11 shows the effect of the inlet combustion gases temperature in the kiln temperature field. It can be observed the same qualitative behavior for all cases, but higher levels are obtained when higher inlet temperatures are used, as expected.

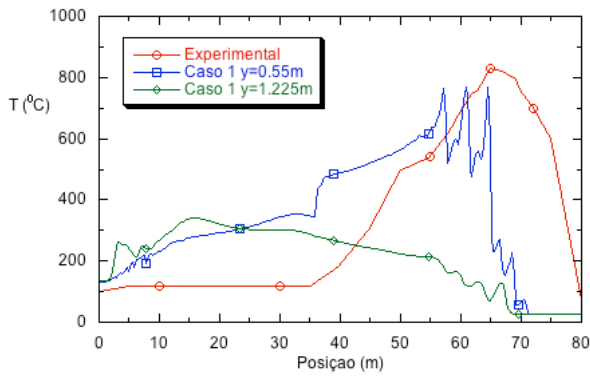


Figure 7. Temperature through the kiln. Comparison with experimental results obtained in Santos, 2001

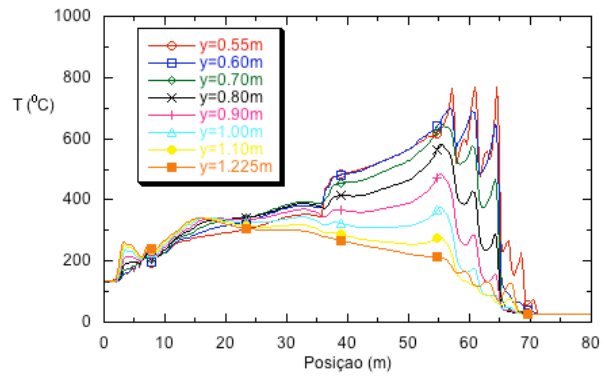


Figure 8. Temperature at different lateral positions, Case 1.

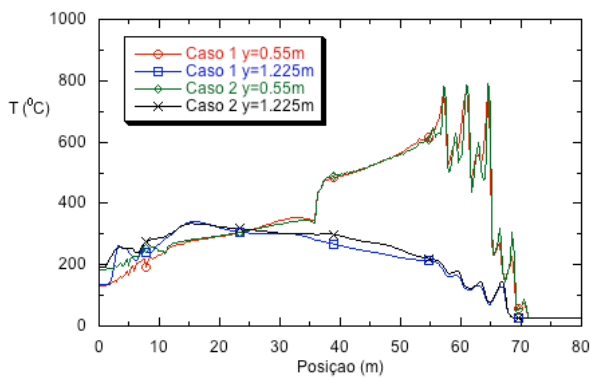


Figure 9. Influence of porosity on temperature field.

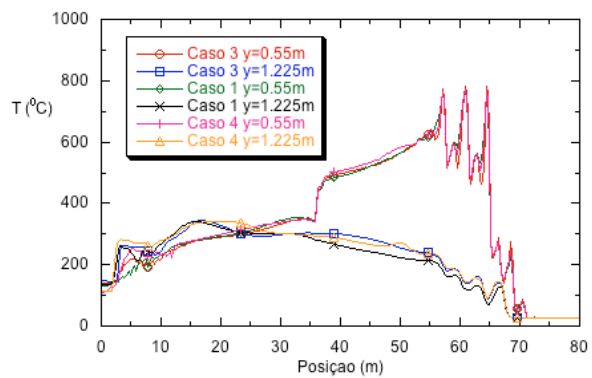


Figure 10. Influence of permeability on temperature field

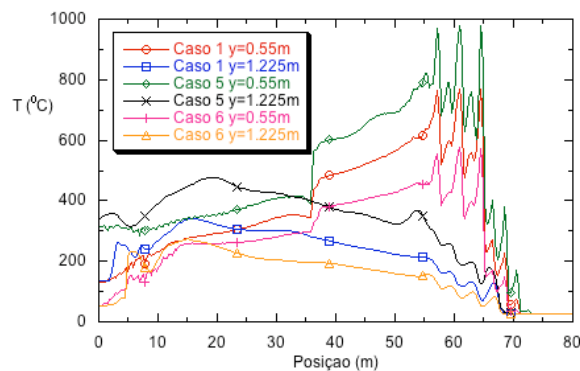


Figure 11. Influence of inlet combustion gases temperature on temperature field

5. Final Remarks

In this work, the temperature and velocity fields inside a simplified tunnel kiln were analyzed numerically using the Fluent software. The conservation equations of mass, momentum and energy were discretized using the finite volume technique. Due to high levels of temperature, radiation heat transfer was considered, and the DTRM (Discret Transfer Radiation Model) model was used. In order to validate the numerical procedure and to evaluate the performance of natural gas as a fuel, instead of sawdust, the results were compared with experimental ones obtained in Santos (2001). A good agreement was obtained, indicating that natural gas can be used as fuel in this kind of kiln. The effects of the load porosity and permeability on temperature fields were investigated and were considered negligible. The effect of inlet combustion gases temperature was also studied, and it was observed that it strongly affects the temperature field inside the kiln.

6. Acknowledgements

The authors thank CNPq, Finep, Petrobras and ANP for the support during the development of this work.

7. References

- Abou-Ziyan, H.Z., 2004, "Convective Heat Transfer from Different Brick Arrangements in Tunnel Kilns", Applied Thermal Engineering, Vol. 24, pp. 171-191.
- Carvalho, M.G., Farias, T., and Fontes, P., 1991, "Predicting Radiative Heat Transfer in Absorbing, Emitting, and Scattering Media Using the Discrete Transfer Method", W.A. Fiveland et al, Fundamentals of Radiation Heat Transfer, ASME HTD, Vol. 160, pp. 17-26.
- Carvalho, M.G. and Nogueira, M., 1997, "Improvement of Energy Efficiency in Glass-Melting Furnaces, Cement Kilns and Baking Ovens, Applied Thermal Engineering, Vol. 17, pp. 921-933.
- Essenhigh, R.H., 2001, "Studies in Furnace Analysis: Prediction of Tunnel Kiln Performance by Application of the Integral Energy Equation", Energy & Fuels, Vol. 15, pp. 552-558.
- Fluent Users Guide, 2004, Fluent Inc.
- Santos, G.M., 2001, "Study of thermal behavior of a tunnel kiln used in red ceramic industry", Master Thesis, Federal University of Santa Catarina, Santa Catarina, Brazil. (in portuguese)

8. Responsibility notice

The authors are the only responsible for the printed material included in this paper.